

## Directing Brownian Motion on a Periodic Surface

David Speer,<sup>1</sup> Ralf Eichhorn,<sup>1,2</sup> and Peter Reimann<sup>1</sup>

<sup>1</sup>Universität Bielefeld, Fakultät für Physik, 33615 Bielefeld, Germany

<sup>2</sup>NORDITA, Roslagstullsbacken 23, 10691 Stockholm, Sweden

(Received 14 January 2009; published 26 March 2009)

We consider an overdamped Brownian particle, exposed to a two-dimensional, square lattice potential and a rectangular ac drive. Depending on the driving amplitude, the linear response to a weak dc force along a lattice symmetry axis consist in a mobility in basically any direction. In particular, motion exactly opposite to the applied dc force may arise. Upon changing the angle of the dc force relatively to the square lattice, the particle motion remains predominantly opposite to the dc force. The basic physical mechanism consists in a spontaneous symmetry breaking of the unbiased deterministic particle dynamics.

DOI: 10.1103/PhysRevLett.102.124101

PACS numbers: 05.45.-a, 05.40.-a, 05.60.-k

Brownian particle dynamics in two-dimensional periodic potential landscapes arise in a large variety of different contexts. Examples include driven vortex lattices [1–3], surface diffusion [4], a ring of several Josephson junctions [5], colloidal particles or globular DNA in structured microfluidic devices [6,7] and in optical [8,9] or magnetic [10] lattices, enzymatic reaction cycles driving molecular motors [11], nanoscale friction [12] and superlubricity [13]. They have recently attracted considerable theoretical [1,14] and experimental [8] interest for particle sorting in two-dimensional periodic structures with the help of an externally applied dc force, whose angle relatively to the periodic potential can be parametrically changed. The key point is that the resulting particle velocity may exhibit a different direction than the applied dc force and that the deflection angle may be different for different particle species. While the deflection angles between force and velocity remain bounded to relatively small values, our present system will lead to (practically) arbitrary deflection angles.

A second recent series of papers [2,10] consider the same system but in the presence of an additional circular ac drive. Deflection angles up to 90° (absolute transverse mobility) have been found in [2], while [10] reports transporting orbits in the absence of a dc drive. A related variant is to replace the circular by a more common, linear ac drive, but now breaking the time-space symmetry by choosing a bi-harmonic driving signal [3], and focusing on the low friction regime [15]. The setup we will consider here is related but simpler: a standard ac drive without any concomitant space-time symmetry breaking and negligible inertia effects.

The unbiased far from equilibrium dynamics of a Brownian particle, responding to a dc force by a directed transport opposite to that force, have been extensively investigated under the label “absolute negative mobility” (ANM) [7,16]. Our present work represents the natural extension, namely, an unbiased far from the equilibrium system admitting an easily controllable linear response into

(practically) any direction relative to the dc force, including ANM as a special case.

We consider the following 2D Langevin dynamics of a Brownian particle with coordinates  $\vec{r} = x\vec{e}_x + y\vec{e}_y$ :

$$\dot{\vec{r}}(t) = A(t)\vec{e}_\alpha + F\vec{e}_\phi - \vec{\nabla}U(\vec{r}(t)) + \sqrt{2\Gamma}\vec{\xi}(t). \quad (1)$$

Thus, inertia effects are neglected (overdamped dynamics), and the friction coefficient is absorbed into the time unit. As illustrated with Fig. 1,  $A(t)$  is the ac-driving signal along the direction  $\vec{e}_\alpha := (\cos\alpha, \sin\alpha)$ , and analogously for the dc-bias  $F\vec{e}_\phi$ . The periodic potential is represented by  $U(\vec{r})$  and thermal fluctuations of temperature  $\Gamma$  are modeled by the two delta-correlated, Gaussian noise components of  $\vec{\xi}(t)$ . We focus on the particularly simple rectangular driving  $A(t) = a\text{sign}\{\cos(\Omega t)\}$  with amplitude  $a$  and period  $T = 2\pi/\Omega$ . We verified that a sinusoidal  $A(t)$  leaves all

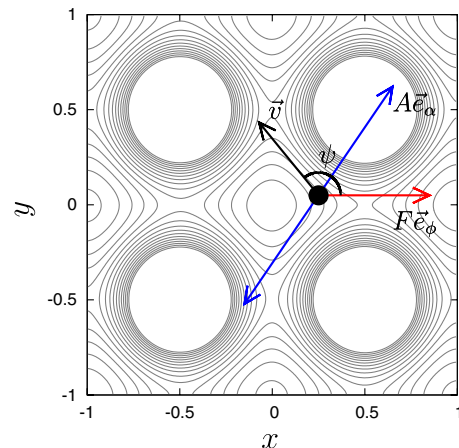


FIG. 1 (color online). Schematic illustration of our model (1). The contour lines represent the potential  $U(\vec{r})$  with a cutoff for better visualization (white discs). The double arrow indicates the ac-drive  $A(t)\vec{e}_\alpha$ , one arrow the dc-bias  $F\vec{e}_\phi$ , and another arrow the particle velocity (2). The particle is sketched by the black dot. The angle  $\psi$  quantifies the “deflection” of  $\vec{v}$  from  $F\vec{e}_\phi$ .

our main findings qualitatively unchanged and expect the same for even more general  $A(t)$ . Further, we focus on the potential  $U(\vec{r}) = \sum \tilde{U}(\vec{r} + Ln\vec{e}_x + Lm\vec{e}_y)$  with  $r := |\vec{r}|$ ,  $\tilde{U}(\vec{r}) = u \exp\{-r/\lambda\}/r$ , and  $u, \lambda > 0$ . In other words, we consider a square lattice of repulsive Yukawa potentials, a standard choice for screened charges [2]. Again, we expect that our results remain qualitatively unchanged for more general  $\tilde{U}(\vec{r})$ , modelling, e.g., pinned vortices [1], optical tweezers [8,9], or magnetic bubbles [10], and we have explicitly verified this for Gaussian shaped repulsive and attractive potentials. Without loss of generality we chose length and time units with  $L = 1$  and  $u = 1$ . Regarding  $\lambda$ , we obtained practically indistinguishable results for all  $\lambda \geq 4$ , variations by a few percent down to  $\lambda \approx 1$ , and notable quantitative but no qualitative differences at least down to  $\lambda \approx 0.1$ . In the following we focus on the representative example  $\lambda = 4$ .

The observable of main interest will be the time-averaged particle velocity

$$\vec{v} = v_x \vec{e}_x + v_y \vec{e}_y := \lim_{t \rightarrow \infty} \frac{1}{t} \int_0^t dt' \dot{\vec{r}}(t'), \quad (2)$$

being independent of the seed  $\vec{r}(0)$  and the realization of  $\tilde{\xi}(t)$  in (1) for any  $\Gamma > 0$  due to ergodicity reasons.

Generally speaking, the periodic potential, the ac drive and the dc bias in (1) give rise to several “competing directions”, whose net effect on the velocity  $\vec{v}$  from (2) is far from obvious. For zero bias  $F$ , the ac forcing still keeps the system off equilibrium but any nonzero velocity  $\vec{v}$  is prohibited by symmetries [17]. Our first objective is the linear response of  $\vec{v}$  to a weak dc bias along the  $x$  axis, cf. Fig. 1. Our findings in Fig. 2 exhibit a quite intriguing behavior. Keeping all “competing directions” fixed and solely changing the ac amplitude by 40%, almost any direction of  $\vec{v}$  may arise, even motion exactly opposite to the applied dc bias (ANM).

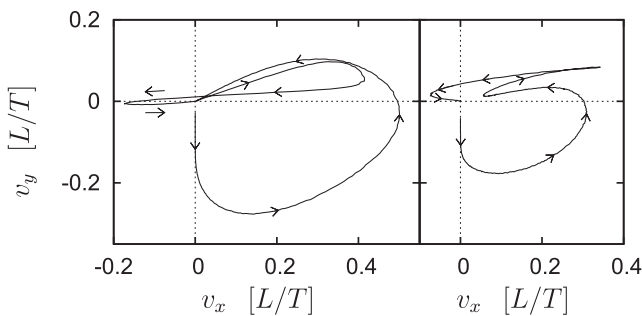


FIG. 2. Velocity (2) from numerical simulations of (1) for  $\alpha = 0.15 \cdot 360^\circ = 54^\circ$ ,  $a \in [4.3, 8]$ ,  $\phi = 0^\circ$ ,  $F = 0.03$ ,  $\Omega = 4.3$ ,  $\Gamma = 2.2 \cdot 10^{-4}$  (left) and  $\Gamma = 6.7 \cdot 10^{-4}$  (right). Shown is the parametric dependence of the velocity components  $v_x, v_y$  on the ac-amplitude  $a$  in units of  $L/T$  ( $L = 1$ ,  $T = 2\pi/\Omega$ ). Arrows indicate increasing  $a$  values. Upon further decreasing  $F$ , a close to linear response behavior of  $\vec{v}$  results (not shown).

Next, we focus on a set of parameters close to the occurrence of ANM in Fig. 2 and now ask for the response of  $\vec{v}$  upon changing the direction of the dc bias. Again, the results in Fig. 3 are quite nontrivial, the most remarkable feature being that the projection of the velocity along the dc bias is mostly negative, i.e., the particle motion remains predominantly opposite to the dc force ( $90^\circ < \psi < 270^\circ$ ). Similarly as in Fig. 2, the effect is particularly striking for small noise strengths  $\Gamma$ , and vanishes for  $\Gamma \geq 10^{-3}$ .

To better understand these findings we first focus on the deterministic dynamics ( $\Gamma = 0$ ) in the simplest case when the ac drive and the dc bias are parallel and acting along one of the main symmetry axes of the periodic potential. Regarding the (1, 0) direction, i.e.,  $\phi = \alpha = 0^\circ$ , the lines  $y = n/2$  constitute invariant sets of the deterministic dynamics (1), stable for odd and unstable for even  $n$ . Thus, the particle motion is confined between two neighboring such lines and generically is attracted by the one with odd  $n$  for large times. Further, the velocity (2) necessarily must follow the direction of the dc force, i.e.,  $\psi = 0^\circ$ , and, in particular, vanishes for  $F = 0$ . This qualitative behavior remains unchanged in the presence of noise ( $\Gamma > 0$ ). Analogous conclusions hold for the (0, 1) lattice direction.

Turning to the (1, 1) direction, i.e.,  $\phi = \alpha = 45^\circ$ , the lines  $x - y = n$  now constitute invariant sets of the deterministic dynamics (1) due to its invariance under  $S_1: (x, y) \mapsto (y, x)$ . Again, the particle motion must remain confined between two adjacent such lines, implying for the velocity (2) that  $\psi = 0^\circ$  and hence  $v_x = v_y$ . But now, the motion on the invariant lines may change its stability properties upon variation of a system parameter, and additional nontrivial attractors, not contained in any of the invariant lines, may arise. A typical example is shown in Fig. 4. We see that—depending on the driving amplitude  $a$  and possibly also on the seed  $\vec{r}(0)$ —the orbit  $\vec{r}(t)$  approaches a periodic or a chaotic long time behavior. The concomitant velocity (2) is still well defined but—in contrast to the noisy case  $\Gamma > 0$ —now may depend on the initial condition  $\vec{r}(0)$ . The “central” straight line in the bifurcation diagram for  $a < 3.22$  belongs to all the periodic attractors on the invariant sets  $x - y = n$ , exemplified by

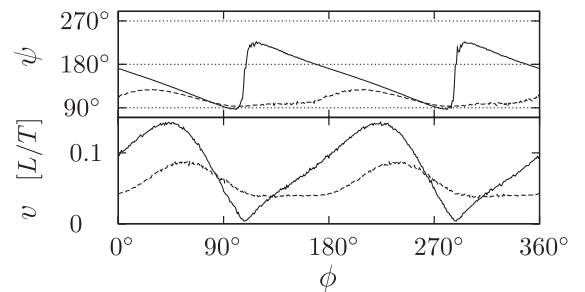


FIG. 3. Deflection angle  $\psi$  (see Fig. 1) and velocity  $v := |\vec{v}|$  versus “dc directionality”  $\phi$  [see (1)] for the same system as in Fig. 2 but with  $a = 7.4$ , and  $\Gamma = 4.4 \cdot 10^{-4}$  (solid),  $\Gamma = 6.7 \cdot 10^{-4}$  (dashed).

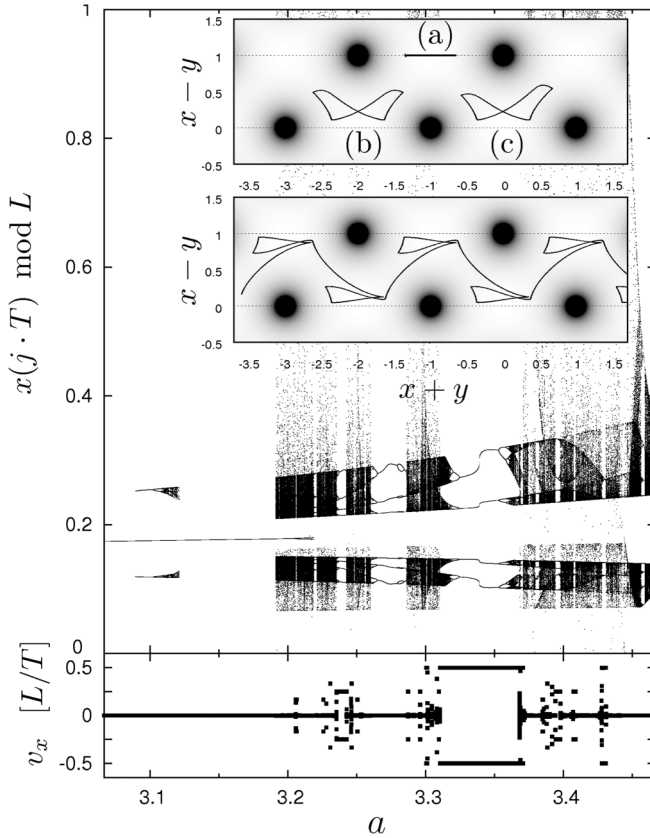


FIG. 4. Upper part: Bifurcation diagram for the unbiased ( $F = 0$ ) deterministic ( $\Gamma = 0$ ) dynamics (1) with  $\alpha = 45^\circ$ ,  $\Omega = 3$ , and varying  $a$ . Shown is a stroboscopic representation of the attractors, governing the long-time behavior, by plotting  $x(jT)$  modulo  $L$  ( $L = 1$ ), i.e., the reduced  $x$  component at multiples  $j$  of the driving period  $T = 2\pi/\Omega$ , for several different seeds  $\vec{r}(0)$  after initial transients have died out. Lower part: Corresponding  $x$  component of the average velocity (2) in units of  $L/T$ . Upper inset: Stable periodic orbits (attractors) for  $a = 3.1$  (a and b) and for  $a = 3.107$  (c). Dotted horizontal lines: invariant sets  $x - y = n$ . Black “clouds” and “discs” represent the potential  $U(\vec{r})$ , corresponding to Fig. 1 after a  $45^\circ$  rotation. Lower inset: stable period-2 transporting orbit for  $a = 3.33$ .

(a) in the upper inset of Fig. 4, and giving rise to a vanishing average velocity. At  $a \approx 3.09$  we observe the appearance of an additional pair of nontransporting ( $\vec{v} = \vec{0}$ ) periodic attractors, spontaneously breaking  $S_1$  as well as the second symmetry  $S_2: (x, y) \mapsto (-x, -y)$  of (1), but still maintaining (up to translations)  $S_1 \circ S_2: (x, y) \mapsto (-y, -x)$ , see (b) in Fig. 4. Thus, there are now three coexisting attractors within every unit cell of the periodic potential, one of type (a), the others of type (b) and its image under  $S_1$ . At  $a \approx 3.102$  the pair of type (b) attractors exhibit a pitchfork bifurcation, which spontaneously breaks the  $S_1 \circ S_2$  symmetry (symmetry breaking bifurcation [18]), resulting in four distinct, nontransporting attractors per unit cell. One of them is exemplified with (c) in Fig. 4, its three “brothers” follow as mirror images with

respect to the closest  $x - y = n$  and/or  $x + y = n$  lines. Upon further increasing  $a$ , a period doubling route to chaos follows, which would be impossible without the preceding symmetry breaking bifurcation [18]. The corresponding attractors lose stability by way of a crisis at  $a \approx 3.12$ . They reappear beyond  $a \approx 3.19$  as “chaotic bands”, interrupted by “periodic windows”. Some of these windows exhibit attractors corresponding to phase-locked *transporting* orbits. The symmetry breaking bifurcation at  $a \approx 3.102$  is pivotal for such transporting orbits: Since there is no systematic force ( $F = 0$ ), which could favor motion in one or the other direction, *spontaneous symmetry breaking* of all symmetries involving  $S_2$  is an indispensable prerequisite for transporting orbits. The simplest and most prominent example arises within the periodic window at  $a \approx 3.33$ , exhibiting two attractors between any pair of adjacent  $x - y = n$  lines. One such orbit is exemplified in the lower inset of Fig. 4, its “twin brother” follows as mirror image with respect to any  $x + y = n$  line. Apparently, this orbit arises by continuing the deformation of orbit (b), which leads to (c) even further, and rewiring one of its “arms” into the neighboring unit cell. The latter operation cannot be realized by a continuous deformation and hence one might guess that this somehow happens within the “gap” in the bifurcation diagram between  $a \approx 3.12$  and  $a \approx 3.19$ .

Because of the  $S_1 \circ S_2$  symmetry at  $F = 0$ , oppositely transporting orbits coexist and are stable within exactly the same range of the other system parameters. Applying a force  $F \neq 0$ , however, breaks the symmetry and hence the existence regions of the two orbits in parameter space no longer coincide. Closer inspection of how these regions change shape and size reveals that there are, for not too large  $|F|$ , parameter values, where *the only stable orbit is the one which transports against the dc-bias  $F$* . In other words, we recover yet another example of “pure” ANM ( $\psi = 180^\circ$ ) [7,16], which furthermore turns out to survive even in the presence of (sufficiently weak) noise ( $\Gamma > 0$ ).

We finally address the case of arbitrary (but fixed) orientations of the external forcings. Without loss of generality we restrict ourselves to  $0 < \alpha < 90^\circ$  but admit arbitrary  $\phi$ . For such general driving directions the deterministic dynamics (1) is not restricted any more by simple invariant sets. Rather, by means of extensive computer simulations we have found that transporting particle motion is created in a way very similar to the case exemplified above with Fig. 4, and typically “locks” to one of the three main symmetry axes (1, 0), (0, 1) or (1, 1), depending on amplitude and frequency of the ac drive. In particular, for  $F = 0$ , symmetry dictates the *coexistence of transport into opposite directions* for either of these basic orientations. Applying a (not too large) dc-bias  $F\vec{e}_\phi$  along a direction that is generally different from the one of the ac drive,  $\phi \neq \alpha$ , has two main effects: First, this coexistence is lifted, yielding parameter regions where only one transporting direction out of the 6 different possible directions is stable.

Second, new transport directions around the orientation of the bias force become accessible and follow a similar “locking scheme” as in [14] upon variation of a system parameter.

In other words, systematically changing, say, the driving amplitude  $a$  leads to “jumps” in the deterministic transport direction where—due to the time-dependent ac drive—also transport with velocity components opposite to the bias force occurs, in marked contrast to previous findings in [14]. The main effect of (weak) thermal noise is to “interpolate” between neighboring deterministic directions, resulting in the smooth behavior shown in Fig. 2: transport in virtually any direction but with emphasis on directions around the orientation of the dc bias. Similarly, the variations of the deflection angle  $\psi$  observed in Fig. 3 result from a basically unchanged orientation of  $\vec{v}$  into the “negative” (1, 0) direction as long as the dc bias has a non-vanishing component in the “positive” (1, 0) direction (i.e.,  $-90^\circ \leq \phi \leq 90^\circ$ ) and a quick transition into the opposite situation when the dc orientation  $\phi$  moves into the complementary regime between  $90^\circ$  and  $270^\circ$ . In any case, noise strengths  $\Gamma$  that are too large basically override the effects of the periodic potential and the system tends to return to the trivial behavior in the absence of the periodic potential.

In conclusion, several quite astonishing linear response transport phenomena of a very simple and general non-equilibrium system have been observed and understood to the extent that an efficient and systematic search of pertinent parameter regions becomes easily feasible. The system is minimal in so far as any further reduction or simplification unavoidably rules out one of the indispensable prerequisites, most notably the occurrence of spontaneous symmetry breaking and chaos in the deterministic limit. On the other hand, the effects are robust against a large variety of modifications and amendments of the model and hence should be realizable in several different experimental systems [5–10], for instance for particle sorting purposes.

We thank J. Nagel, D. Koelle, and R. Kleiner for fruitful discussions. This work was supported by Deutsche Forschungsgemeinschaft under SFB 613 and RE1344/4-1.

---

[1] C. Reichhardt and F. Nori, Phys. Rev. Lett. **82**, 414 (1999); B. Y. Zhu, F. Marchesoni, V. V. Moshchalkov, and F. Nori, Phys. Rev. B **68**, 014514 (2003).  
 [2] C. Reichhardt, C. J. Olson, and M. B. Hastings, Phys. Rev. Lett. **89**, 024101 (2002); C. Reichhardt and C. J. Olson Reichhardt, Phys. Rev. E **68**, 046102 (2003).  
 [3] S. Ooi, S. Savel'ev, M. B. Gaifullin, T. Mochiku, K. Hirata, and F. Nori, Phys. Rev. Lett. **99**, 207003 (2007).

[4] J. L. Vega, R. Guantes, and S. Miret-Artés, J. Phys. Condens. Matter **14**, 6193 (2002); S. Miret-Artés and E. Pollak, J. Phys. Condens. Matter **17**, S4133 (2005).  
 [5] U. Geigenmüller, J. Appl. Phys. **80**, 3934 (1996); A. Sterck, S. Weiss, and D. Koelle, Appl. Phys. A **75**, 253 (2002).  
 [6] C.-F. Chou *et al.*, Proc. Natl. Acad. Sci. U.S.A. **96**, 13 762 (1999); R. L. Huang *et al.*, Nat. Biotechnol. **20**, 1048 (2002); Science **304**, 987 (2004); M. Baba *et al.*, Appl. Phys. Lett. **83**, 1468 (2003); E. B. Cummings and A. K. Singh, Anal. Chem. **75**, 4724 (2003); J. Regtmeier *et al.*, Anal. Chem. **79**, 3925 (2007).  
 [7] A. Ros *et al.*, Nature (London) **436**, 928 (2005); J. Regtmeier *et al.*, J. Sep. Sci. **30**, 1461 (2007); Eur. Phys. J. E **22**, 335 (2007).  
 [8] P. T. Korda, M. B. Taylor, and D. G. Grier, Phys. Rev. Lett. **89**, 128301 (2002); M. P. MacDonald, G. C. Spalding, and K. Dholakia, Nature (London) **426**, 421 (2003); P. Tierno, A. Soba, T. H. Johansen, and F. Sagués, Appl. Phys. Lett. **93**, 214102 (2008).  
 [9] K. Mangold, P. Leiderer, and C. Bechinger, Phys. Rev. Lett. **90**, 158302 (2003); S. Beil *et al.*, Europhys. Lett. **73**, 450 (2006).  
 [10] P. Tierno, T. H. Johansen, and T. M. Fischer, Phys. Rev. Lett. **99**, 038303 (2007); A. Soba, P. Tierno, T. M. Fischer, and F. Sagués, Phys. Rev. E **77**, 060401(R) (2008).  
 [11] M. O. Magnasco, Phys. Rev. Lett. **72**, 2656 (1994); P. Reimann Phys. Rep. **361**, 57 (2002).  
 [12] R. Prioli, A. M. F. Rivas, F. L. Freire, Jr., and A. O. Caride, Appl. Phys. A **76**, 565 (2003); P. Reimann and M. Evstigneev, New J. Phys. **7**, 25 (2005).  
 [13] M. Dienwiebel *et al.*, Phys. Rev. Lett. **92**, 126101 (2004); G. S. Verhoeven, M. Dienwiebel, and J. W. M. Frenken, Phys. Rev. B **70**, 165418 (2004).  
 [14] A. Gopinathan and D. G. Grier, Phys. Rev. Lett. **92**, 130602 (2004); C. Reichhardt and C. J. Olson Reichhardt, Phys. Rev. E **69**, 041405 (2004); M. Pelton, K. Ladavac, and D. G. Grier, Phys. Rev. E **70**, 031108 (2004); A. M. Lacasta, J. M. Sancho, A. H. Romero, and K. Lindenberg, Phys. Rev. Lett. **94**, 160601 (2005); J. P. Gleeson, J. M. Sancho, A. M. Lacasta, and K. Lindenberg, Phys. Rev. E **73**, 041102 (2006).  
 [15] R. Guantes and S. Miret-Artés, Phys. Rev. E **67**, 046212 (2003); S. Sengupta, R. Guantes, S. Miret-Artés, and P. Hänggi, Physica (Amsterdam) **338A**, 406 (2004).  
 [16] R. Eichhorn, P. Reimann, and P. Hänggi, Phys. Rev. Lett. **88**, 190601 (2002); Phys. Rev. E **66**, 066132 (2002); B. Cleuren and C. Van den Broeck, Phys. Rev. E **67**, 055101 (R) (2003); L. Machura, M. Kostur, P. Talkner, J. Luczka, and P. Hänggi, Phys. Rev. Lett. **98**, 040601 (2007); M. Kostur, L. Machura, P. Talkner, P. Hänggi, and J. Luczka, Phys. Rev. B **77**, 104509 (2008); D. Speer, R. Eichhorn, and P. Reimann, Europhys. Lett. **79**, 10005 (2007); Phys. Rev. E **76**, 051110 (2007); J. Nagel *et al.*, Phys. Rev. Lett. **100**, 217001 (2008).  
 [17] S. Denisov, Y. Zolotaryuk, S. Flach, and O. Yevtushenko, Phys. Rev. Lett. **100**, 224102 (2008).  
 [18] J. W. Swift and K. Wiesenfeld, Phys. Rev. Lett. **52**, 705 (1984).